Pramana – J. Phys. (2022) 96:99
https://doi.org/10.1007/s12043-022-02342-x

Hydromagnetic free convection in a vertical channel with induced magnetic field: Open and short circuits

NAVEEN DWIVEDI[1],*, ASHOK KUMAR SINGH[1], PALLATH CHANDRAN[2] and NIRMAL C SACHETI[2,3]

[1]Department of Mathematics, Institute of Science, Banaras Hindu University, Varanasi 221 005, India
[2]Department of Mathematics, College of Science, Sultan Qaboos University, Al Khod PC 123, Muscat, Sultanate of Oman
[3]153, Arabella 2, Mudon Community, P.O. Box 939571, Dubai, United Arab Emirates
*Corresponding author. E-mail: naveen.dwivedi5@bhu.ac.in

MS received 25 July 2020; revised 29 December 2021; accepted 29 December 2021

Abstract. This theoretical paper deals with a fully developed free convective flow of an incompressible viscous and electrically conducting fluid in an infinitely long rigid vertical channel in the presence of an externally applied magnetic field. By retaining the induced magnetic field, we have carried out a detailed analysis of the field equations and obtained a host of interesting results corresponding to both open-circuit and short-circuit arrangements. The governing PDEs, which under the chosen physical configuration get transformed to a set of ordinary differential equations together with appropriate boundary conditions, have further been subjected to non-dimensionalisation. Using the theory of simultaneous ordinary differential equations, the analytical solutions for velocity, temperature field and induced magnetic field were obtained. These solutions were used to obtain important quantities of engineering interest such as current density, wall skin friction and volumetric flux for both open and short circuits. The effect of Hartmann number on the velocity, induced magnetic field and induced current density were shown quite extensively. Furthermore, the results for the symmetric and asymmetric heating of the vertical walls of the channel for open- and short-circuit arrangements were compared. It is found that for the open-circuit arrangement, the velocity, induced current density and induced magnetic field are higher than that for the short-circuit arrangement.

Keywords. Vertical channel; transverse magnetic field; induced magnetic field; symmetric and asymmetric heating; induced current density; wall skin friction.

PACS Nos **44.25.+f; 47.10.A−; 47.15.−X; 47.65.−d; 52.65.Kj**

1. Introduction

The analyses of free convection, forced convection and mixed convection are active and interesting areas of fluid dynamical research due to a large number of applications in engineering and industry. The literature on the study of such convective flows is exhaustive. In the case of free convective flows, there arises a coupling of the thermal and momentum transport processes; and this renders solving the governing equations rather tedious and generally much less amenable to analytical treatments. When the fluid flow is subjected to additional external forces such as applied magnetic field, the governing equations are further modified due to the presence of Maxwell's equations. Magnetohydrodynamic (MHD) flows in different geometries, under an applied external magnetic field, have been reported in the literature for several decades due to wide-ranging real-life applications in several areas such as MHD power generator, nuclear fuel debris treatment, solar power collector, to name a few. Further applications of MHD are also found in medical science and biological systems, e.g., magnetic drug targeting, cancer tumour treatment, magnetic devices for cell separation, magnetotherapy, control of gastrointestinal disorders, magnetic endoscopy, magnetic resonance imaging (MRI), transport of complex biowaste fluids etc. In manufacturing processes in industries, MHD flows are encountered, for example, in the production of lead/lithium eutectic alloys. Further, applications of such flows have been reported in important fields like chemical and metallurgical engineering, astrophysics,

Published online: 16 May 2022

agriculture, geophysics, oceanography and geothermal power generation. Also, magnetohydrodynamic sensors are known to provide correct measurements of angular velocities in inertial navigation systems.

Given the multifaceted applications of MHD flows, free convection studies in the presence of an applied magnetic field, under a host of assumptions/idealisations, have been carried out by a large number of researchers for both steady and unsteady flows. One of the common assumptions made in the free convection analyses relates to the neglection of the induced magnetic field in the flow field which notably is justifiable for only low magnetic Reynolds number flows. It appears that such restrictions have often been imposed by a vast body of theoretical researchers to simplify the governing flow equations and their solutions. However, it is worth mentioning that in many real-life applications, such an assumption is too restrictive, and thus one should consider the presence of the induced magnetic field beside the externally applied one. Although many studies are reported in literature dealing with both cases, the investigations of the latter type are relatively much less exhaustive than the former ones. In the present work, we have therefore analysed a special type of MHD convective flow which corresponds to free convection in a vertical channel in the presence of an induced field, subject to both open-circuit and short-circuit arrangements.

A fairly large number of investigations have been reported in the literature concerning free convection in electrically conducting viscous incompressible fluids in the presence of vertical plane rigid boundaries. One of the early studies on this topic can be traced to the work of Sparrow and Cess [1]. In later years, several studies appeared in literature dealing with MHD free convective flows involving infinitely long bounding vertical plates or through channels. Restricting ourselves mainly to the developments in this area during the recent decades, we set out to quote some relevant works. For instance, Sacheti *et al* [2] and Chandran *et al* [3] analysed unsteady free convective flow induced by a vertically moving infinite plate assuming constant heat flux at the bounding plate. They showed that the increase in the velocity caused by the larger heat flux can be checked by increasing the intensity of the applied magnetic field. Singer [4] investigated the effect of forced and free convection and heat transfer through a vertical channel in the presence of an applied magnetic field. An unsteady natural convective flow and heat transfer in a porous channel has been discussed by Chamkha [5]. Han [6] investigated the impact of magnetic field on the natural convective flow of a radiating and electrically conducting fluid in an enclosure. The work of Umavathi and Liu [7] studied heat transfer in the mixed convective flow of an incompressible viscous and electrically conducting fluid in a vertical channel in the presence of a heat source/sink. Jha and Apere [8] analysed an unsteady free convective flow in a vertical channel with porous walls in the presence of an applied magnetic field assuming one of the walls is moving with a constant velocity. In a subsequent study, Jha *et al* [9] considered the convective flow in a vertical microchannel by applying a magnetic field perpendicular to the microchannel. Sheikholeslami *et al* [10] investigated the effect of heat transfer as well as thermal radiation on nanofluid flow in an enclosure due to a constant heating flux element. Recently, Dwivedi *et al* [11], Dwivedi and Singh [12,13], Mathur and Mishra [14], Ghosh and Mukhopadhyay [15] have examined the hydromagnetic free convective flow of incompressible viscous fluids in various geometries. However, all these flow problems have been analysed by neglecting the induced magnetic field.

As mentioned earlier, there are many applications involving hydromagnetic flows where the induced magnetic field cannot be neglected. Taking into account the presence of an induced magnetic field, in one of the earlier studies, Globe [16] investigated the effect of radial magnetic field on the steady flow of an incompressible electrically conducting fluid in an annular channel. Yen [17] analysed the effect of uniform magnetic field on electrically conducting fluid flow in channels with heat transfer and constant wall heat flux. Arora and Gupta [18] discussed the effect of radial magnetic field on electrically conducting and viscous incompressible fluid flow between two rotating coaxial cylinders. Guria *et al* [19] considered the MHD flow of electrically conducting and viscous incompressible fluid between vertical walls with wall conductance. Singh *et al* [20] investigated numerically the effect of induced magnetic field on free convective flow through vertical channels and discussed many physical cases of interest. Further studies involving induced magnetic fields in free convective flows under different physical configurations have been reported by many researchers [21–30].

In this work, we consider the two-dimensional fully developed steady laminar flow of an incompressible, electrically conducting fluid, with constant viscosity and constant electrical conductivity, between two infinitely long vertical non-conducting walls with open-circuit and short-circuit arrangements. For the rectangular coordinate system $oxyz$, the vertical x-axis is chosen along the direction of the flow while the applied magnetic field is in the z-direction. Furthermore, we assume that electrodes are connected in the y-direction. In an open-circuit arrangement, the electrodes are left unconnected and so the currents return through the fluid only in yz plane and there is no externally applied current.

In a short-circuit arrangement, the electrodes are connected by a highly conducting wire and so the potential at the two electrodes is the same and the electric field is zero. Some earlier studies on the effects of open or short circuits on fluid convection may be attributed to Osterle and Young [31] and Poots [32] who studied, respectively, the effect of short-circuited and open-circuited Hartmann flow on the fully developed natural convection between two heated walls. Later on, in an interesting paper, Umavathi [33] compared the effects of both open-circuit and close-circuit cases on the flow between parallel plates maintained at different temperatures, in the presence of uniform magnetic and electric fields. Recently, Umavathi *et al* [34] analysed the effect of electric field on solute dispersion in MHD flow with and without chemical reaction for open- and close-circuit cases. It is worthwhile to mention in passing that although our work is not related to stability analysis of flow for both circuits considered, one may discuss this aspect by following some interesting recent papers (see, for instance [35–38]).

Motivated by some of the aforementioned studies, we have investigated in this work the effect of the induced magnetic field on the natural convective flow of an electrically conducting viscous and incompressible fluid between two infinitely long vertical non-conducting walls with open- and short-circuit arrangements. We have considered the physical model by assuming two cases of boundary conditions. In case (A) (asymmetric heating), the temperatures of both walls are different, $T_h \neq T_c = T_m$. In case (B) (symmetric heating), both the walls have the same temperature, $T_h = T_c$. Here T_m represents a reference temperature. The exact solutions for the fluid velocity, induced magnetic field and temperature field are obtained by solving the non-dimensional set of governing ordinary differential equations subject to non-dimensional boundary conditions. Furthermore, we have derived expressions for the skin friction, volume flow rate and induced current density. Finally, we have shown the variations of velocity, induced magnetic field and induced current density in the vertical channel. Also, computed values of the skin friction and flow rate have been presented in tabular form for both cases of the circuits: open and short. The illustrative figures and the table exhibit variations in the physical quantities corresponding to both symmetric and asymmetric heating. In particular, the influence of the Hartmann number on all these physical and derived quantities has been discussed in detail.

2. Mathematical formulation

The basic magnetohydrodynamic (MHD) equations for fully developed natural convective flow of an incompressible viscous and electrically conducting liquid are

$$\nabla \cdot \mathbf{V} = 0, \tag{1}$$

$$\rho\left(\mathbf{V}\cdot\nabla\right)\mathbf{V} = -\nabla p + \mu\left(\nabla^2\mathbf{V}\right) + \mu_e\left(\mathbf{J}\times\mathbf{H}\right) + \rho\mathbf{g}, \tag{2}$$

$$\nabla\times\left(\mathbf{V}\times\mathbf{H}\right) + \upsilon_H\nabla^2\mathbf{H} = \mathbf{0}, \tag{3}$$

$$\left(\mathbf{V}\cdot\nabla\right)T = \frac{k}{\rho C_p}\left(\nabla^2 T\right), \tag{4}$$

$$\mathbf{J} = \sigma\left(\mathbf{E} + \mu_e\mathbf{V}\times\mathbf{H}\right), \tag{5}$$

$$\nabla\cdot\mathbf{E} = \frac{\rho_e}{\varepsilon},\ \nabla\cdot\mathbf{H} = 0,\ \nabla\times\mathbf{E} = \mathbf{0},\ \nabla\times\mathbf{H} = \mathbf{J}, \tag{6}$$

where $\mathbf{V}$ is the velocity field, ρ is the density of the fluid, μ is the coefficient of viscosity, μ_e is the magnetic permeability, $\mathbf{J}$ is the induced current density field, $\mathbf{H}$ is the magnetic field, $\mathbf{g}$ is the gravitational acceleration, σ is the electrical conductivity, υ_H is the magnetic viscosity $(1/(\sigma\mu_e))$, T is the temperature of the fluid, κ is the thermal conductivity, C_p is the specific heat at constant pressure, $\mathbf{E}$ is the electric field, ρ_e is the charge density, ε is the electrical permittivity.

We consider the steady natural convective flow of an incompressible viscous and electrically conducting liquid between two infinite vertical non-conducting walls under the influence of a uniform applied magnetic field H_0 perpendicular to the walls. The distance between the walls is d and the x-axis is taken vertically upwards along the left wall and the z-axis perpendicular to it into the fluid, while the y-axis is taken normal to the xz plane. In this study, as mentioned earlier, we shall consider two cases of wall heating: asymmetric and symmetric. The heating of the walls leads to convective currents in the vertical channel. In the case of asymmetric heating, we assume that the walls $z = 0$ and $z = d$ are maintained at temperatures T_h and T_c, respectively, where $T_h > T_c$. For symmetric heating, however, the wall temperatures are assumed to be equal. We denote the temperature of the fluid and the plates in the reference state by T_m. As the walls are of an infinite extent, the variables describing the flow will depend only on the transverse coordinate z except for the density in the gravitational force. Thus, the fluid velocity will have only one non-zero component in the x-direction.

The physical configuration of the model is presented in figure 1. Under this set-up, the components along the coordinate axes of velocity $\mathbf{V}$, induced current density $\mathbf{J}$, induced magnetic field $\mathbf{H}$ and electric current $\mathbf{E}$ are

$$\mathbf{V} = (u_x, 0, 0)\,,\quad \mathbf{J} = \left(0, j_y, 0\right),\quad \mathbf{H} = (h_x, 0, H_0)\,,\quad \mathbf{E} = \left(0, E_y, 0\right), \tag{7}$$

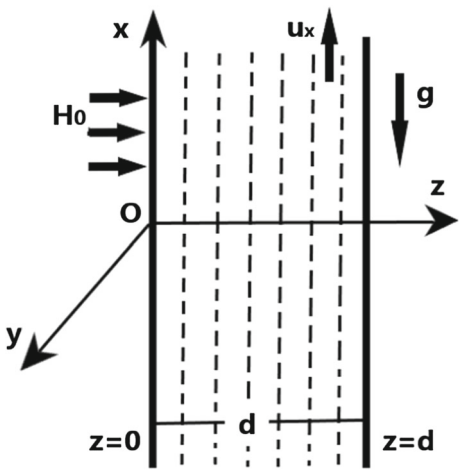

Figure 1. Physical model.

where u_x is the component of the velocity along the x-axis, j_y is the component of the induced current density along the y-axis, h_x is the component of the induced magnetic field along the x-axis and E_y is the component of the electric field along the y-axis.

Assuming the usual Boussinesq approximation, the basic governing equations of viscous, incompressible and electrically conducting fluid with an induced magnetic field can be re-expressed as

$$\upsilon\frac{\mathrm{d}^2u_x}{\mathrm{d}z^2}+\frac{\mu_e H_0}{\rho}\frac{\mathrm{d}h_x}{\mathrm{d}z}+\beta g\,(T-T_m)=0, \tag{8}$$

$$\frac{\mathrm{d}^2h_x}{\mathrm{d}z^2}+\sigma\mu_e H_0\frac{\mathrm{d}u_x}{\mathrm{d}z}=0, \tag{9}$$

$$\frac{\mathrm{d}h_x}{\mathrm{d}z}=\sigma\left(E_y-\mu_e H_0 u_x\right), \tag{10}$$

$$\frac{\mathrm{d}^2T}{\mathrm{d}z^2}=0, \tag{11}$$

where β is the thermal expansion coefficient and T_m is the reference temperature.

The boundary conditions for the velocity, induced magnetic field and temperature field are

$$u_x=0,\quad h_x=0,\quad T=T_h,\quad \text{at } z=0; \tag{12}$$

$$u_x=0,\quad h_x=0,\quad T=T_c,\quad \text{at } z=d. \tag{13}$$

Integrating eq. (9) we have

$$\frac{\mathrm{d}h_x}{\mathrm{d}z}+\sigma\mu_e H_0 u_x=\text{const}. \tag{14}$$

Equation (10) can be rewritten as

$$E_y=\mu_e H_0 u_x+\frac{1}{\sigma}\frac{\mathrm{d}h_x}{\mathrm{d}z}. \tag{15}$$

From eqs (14) and (15), we see that

$$E_y=\text{const}. \tag{16}$$

Eliminating $\frac{\mathrm{d}h_x}{\mathrm{d}z}$ between eqs (8) and (10), we get

$$\upsilon\frac{\mathrm{d}^2u_x}{\mathrm{d}z^2}+\frac{\mu_e H_0}{\rho}\sigma(E_y-\mu_e H_0 u_x)+g\beta\,(T-T_m)=0. \tag{17}$$

For obvious reasons, we shall solve the above boundary value problems after setting them in non-dimensional forms. We therefore introduce

$$z^*=\frac{z}{d},\quad u^*=\frac{u_x}{u_0},\quad h^*=\frac{h_x}{H_0},$$
$$u_0=\frac{d^2\rho g\beta\,(T_h-T_m)}{\mu},\quad T^*=\frac{T-T_m}{T_h-T_m}, \tag{18}$$

where d is the distance between the two walls, u^* is the dimensionless velocity component, h^* is the dimensionless induced magnetic field component, T^* is the dimensionless temperature and u_0 is the characteristic velocity.

Using eq. (18) in eqs (9), (11) and (17), we obtain the following non-dimensional equations:

$$\frac{\mathrm{d}^2u^*}{\mathrm{d}z^{*2}}-Ha^2u^*+Ha^2R_E+T^*=0, \tag{19}$$

$$\frac{\mathrm{d}^2h^*}{\mathrm{d}z^{*2}}+R_\sigma\frac{\mathrm{d}u^*}{\mathrm{d}z^*}=0, \tag{20}$$

$$\frac{\mathrm{d}^2T^*}{\mathrm{d}z^{*2}}=0. \tag{21}$$

The boundary conditions become

$$u^*=0,\quad h^*=0,\quad T^*=1\quad \text{at } z^*=0; \tag{22}$$

$$u^*=0,\quad h^*=0,\quad T^*=R\quad \text{at } z^*=1. \tag{23}$$

In eqs (19) and (20), we have introduced some non-dimensional parameters which indicate the relative significance of specific physical phenomena influencing the flow and heat transfer problem. They are

$$R_E=\frac{E_y}{\mu_e H_0 u_0},\quad R_\sigma=u_0\mu_e\sigma d,\quad R=\frac{T_c-T_m}{T_h-T_m},$$
$$Ha=H_0\mu_e d\sqrt{\frac{\sigma}{\mu}}, \tag{24}$$

where R_E is the electric field parameter, R_σ is the magnetic Reynolds number, R is the buoyancy distribution parameter and Ha is the Hartmann number.

2.1 *Solution procedures*

To solve the non-dimensional equations (19)–(21) with boundary conditions (22) and (23), we used the theory of simultaneous ordinary differential equations. The

expressions for the velocity, induced magnetic field and temperature field are

$$u^* = A\cosh(Haz^*) + B\sinh(Haz^*) + \frac{(R-1)\,z^*}{Ha^2} + \frac{1}{Ha^2} + R_E, \tag{25}$$

$$h^* = Cz^* + D - \frac{R_\sigma}{Ha} \times \left[\begin{array}{l} A\sinh(Haz^*) + B\cosh(Haz^*) \\ + \dfrac{(R-1)z^{*^2}}{2Ha} + \left(HaR_E + \dfrac{1}{Ha}\right) z^* \end{array}\right], \tag{26}$$

$$T^* = 1 + (R-1)\,z^*, \tag{27}$$

where A, B, C and D are arbitrary constants which can be determined by using the boundary conditions (22) and (23). They are

$$A = -\left[R_E + \frac{1}{Ha^2}\right],$$

$$B = \frac{(\cosh(Ha) - R)}{Ha^2\sinh(Ha)} + \frac{(\cosh(Ha) - 1)}{\sinh(Ha)}R_E,$$

$$C = R_\sigma\left[\begin{array}{l} \dfrac{Ha\sinh(\mathrm{Ha}) + 2\,(1 - \cosh(Ha))}{Ha\sinh(Ha)}R_E \\ + \dfrac{Ha\sinh(Ha) + 2(1 - \cosh(Ha))}{2Ha^3\sinh(Ha)} \end{array}\right],$$

$$D = R_\sigma\left[\frac{(\cosh(Ha) - R)}{Ha^3\sinh(Ha)} + \frac{(\cosh(Ha) - 1)}{Ha\sinh(Ha)}R_E\right].$$

The net flux of the current over any horizontal cross-section of the vertical channel, $0 \le z^* \le 1$, is given by

$$J_y = \int_0^1 j_y \mathrm{d}z^*, \tag{28}$$

where

$$j_y = \sigma E_y - \sigma\mu_e H_0 u_0 \times \left[\begin{array}{l} A\cosh(Haz^*)\; B\sinh(Haz^*) \\ + \dfrac{(R-1)\,z^*}{Ha^2} + \dfrac{1}{Ha^2} + R_E \end{array}\right].$$

Equation (28) then yields

$$J_y = \sigma E_y - \sigma\mu_e H_0 u_0 \times \left[\begin{array}{l} \dfrac{A\sinh(Ha)}{Ha} + \dfrac{B\,(\cosh(Ha) - 1)}{Ha} \\ + R_E + \dfrac{R+1}{2Ha^2} \end{array}\right]. \tag{29}$$

In the following, we shall obtain the solutions of velocity, induced magnetic field and current density for the MHD convective flow in the channel for the open- and close-circuit arrangements. We shall then derive the expressions for wall skin friction and volumetric flux.

3. Open and closed circuits

In this section, we shall obtain the expressions for the field variables – velocity, induced magnetic field and induced current density – corresponding to the open- and close-circuit arrangements. We shall also obtain expressions for the skin friction at both walls and the volumetric flow rate through any transverse cross-section of the vertical channel for both these cases.

3.1 *Open-circuit arrangement*

In an open-circuit arrangement, the net flux of the current through the horizontal section of the channel is zero. Thus, from eq. (29) we obtain the result

$$R_E = -\frac{(1+R)}{2Ha^2} - \frac{(1+R)\sinh Ha}{4Ha\,(1-\cosh Ha)}. \tag{30}$$

Using eq. (30), we obtain the expressions for the velocity and induced magnetic field for the open-circuit arrangement as

$$u^* = \left[\frac{(R+1)\sinh(Ha)}{4Ha\,(1-\cosh(Ha))} + \frac{(R-1)}{2Ha^2}\right] \times \cosh(Haz^*) + \left[\frac{(1-R)\,(\cosh(Ha)+1)}{2Ha^2\sinh(Ha)} + \frac{(R+1)}{4Ha}\right] \times \sinh(Haz^*) + \frac{(R-1)}{Ha^2}z^* - \frac{(R+1)\sinh(Ha)}{4Ha(1-\cosh(Ha))} + \frac{(1-R)}{2Ha^2}, \tag{31}$$

$$h^* = R_\sigma\left[\frac{(1-R)\,(\cosh(Ha)+1)}{2Ha^3\sinh(Ha)} + \frac{(R+1)}{4Ha^2}\right] - R_\sigma\left[\frac{(R+1)\sinh(Ha)}{4Ha^2\,(1-\cosh(Ha))} - \frac{(R-1)}{2Ha^3}\right] \times \sinh\left(Haz^*\right) - R_\sigma\left[\frac{(1-R)\,(\cosh(Ha)+1)}{2Ha^3\sinh(Ha)} + \frac{(R+1)}{4Ha^2}\right] \times \cosh\left(Haz^*\right) - R_\sigma\left[\frac{1}{Ha^2}z^* + \frac{(R-1)}{2Ha^2}z^{*^2}\right]. \tag{32}$$

Using eq. (32), the expression for the induced current density, in non-dimensional form, is

$$j^* = -\frac{\mathrm{d}h^*}{\mathrm{d}z^*} = R_\sigma\left[\frac{1}{Ha^2} - \frac{(1-R)}{Ha^2}z^*\right] + R_\sigma\left[\frac{(R+1)\sinh(Ha)}{4Ha\,(1-\cosh(Ha))} + \frac{(R-1)}{2Ha^2}\right] \times \cosh\left(Haz^*\right) + R_\sigma\left[\frac{(1-R)\,(\cosh(Ha)+1)}{2Ha^2\sinh(Ha)} + \frac{(R+1)}{4Ha}\right] \times \sinh\left(Haz^*\right). \tag{33}$$

One of the important quantities of interest in engineering applications of fluid motion is related to the wall skin friction τ. For the present case, the skin friction on the vertical boundaries $z^* = 0$ and at $z^* = 1$, are

$$(\tau)_{z^*=0} = \left(\frac{\mathrm{d}u^*}{\mathrm{d}z^*}\right)_{z^*=0} = \frac{(1-R)\,(\cosh(Ha)+1)}{2Ha\sinh(Ha)} + \frac{(R-1)}{Ha^2} + \frac{(R+1)}{4}, \tag{34}$$

$$(\tau)_{z^*=1} = \left(\frac{\mathrm{d}u^*}{\mathrm{d}z^*}\right)_{z^*=1} = \frac{(1-R)\,(1+\cosh(Ha))}{2Ha\sinh(Ha)} - \frac{(R+1)}{4} + \frac{(R-1)}{Ha^2}. \tag{35}$$

The volumetric flow rate across any horizontal cross-section is given by

$$Q = \int_{z^*=0}^{z^*=1} u^*\left(z^*\right)\mathrm{d}z^* = -\frac{(R+1)}{2Ha^2} - \frac{(R+1)\sinh(Ha)}{4Ha\,(1-\cosh(Ha))}. \tag{36}$$

3.2 *Short-circuit arrangement*

In a short-circuit arrangement, the potential at the two electrodes is the same and the electric field will be zero. This implies $E_y = 0$ and hence $R_E = 0$. We thus obtain the velocity and induced magnetic field for short-circuit arrangement as

$$u^* = \left[-\frac{1}{Ha^2}\right]\cosh(Haz^*) + \left[\frac{(\cosh(Ha)-R)}{Ha^2\sinh(Ha)}\right]\sinh(Haz^*) + \frac{(R-1)}{Ha^2}z^* + \frac{1}{Ha^2}, \tag{37}$$

$$h^* = R_\sigma\left[\frac{R-\cosh(Ha)}{Ha^3\sinh(Ha)}\right]\cosh(Haz^*) + R_\sigma\left[\frac{1}{Ha^3}\right]\sinh(Haz^*) + R_\sigma\frac{\cosh(Ha)-R}{Ha^3\sinh(Ha)} + R_\sigma\left[\frac{(1+R)\,(1-\cosh(Ha))}{Ha^3\sinh(Ha)} + \frac{(R-1)}{2Ha^2}\right]z^* - R_\sigma\frac{(R-1)}{2Ha^2}z^{*^2}. \tag{38}$$

The expression for the induced current density becomes

$$j^* = -\frac{\mathrm{d}h^*}{\mathrm{d}z^*} = -R_\sigma\left[\frac{1}{Ha^2}\right]\cosh(Haz^*) - R_\sigma\left[\frac{\cosh(Ha)-R}{Ha^2\sinh(Ha)}\right]\sinh(Haz^*) + R_\sigma\frac{(R-1)}{Ha^2}z^* + R_\sigma\left[\frac{(R-1)}{2Ha^2} + \frac{(1+R)\,(1-\cosh(Ha))}{Ha^3\sinh(Ha)}\right]. \tag{39}$$

We can obtain the skin friction and flow rate for the short-circuit arrangement very similar to the open-circuit one. These are given by

$$(\tau)_{z^*=0} = \left(\frac{\mathrm{d}u^*}{\mathrm{d}z^*}\right)_{z^*=0} = \frac{(\cosh(Ha)-R)}{Ha\sinh(Ha)} + \frac{(R-1)}{Ha^2}, \tag{40}$$

$$(\tau)_{z^*=1} = \left(\frac{\mathrm{d}u^*}{\mathrm{d}z^*}\right)_{z^*=1} = \frac{(1-R\cosh(Ha))}{Ha\sinh(Ha)} + \frac{(R-1)}{Ha^2}. \tag{41}$$

$$Q = \int_{z^*=0}^{z^*=1} u^*\left(z^*\right)\mathrm{d}z^* = \frac{(1-\cosh(Ha))(1+R)}{Ha^3\sinh(Ha)} + \frac{(R+1)}{2Ha^2}. \tag{42}$$

4. Results and discussions

In the previous section, we have obtained modified expressions for the field variables consequent to the inclusion of induced magnetic field in the hydrodynamic natural convective flow of a viscous incompressible and electrically conducting fluid in a channel bounded by two vertical impermeable parallel non-conducting infinite walls. We obtained analytical expressions for the main field variables for both open- and short-circuit arrangements.

In this section, our aim will be to illustrate graphically how the main physical variables, namely, fluid velocity, induced magnetic field and induced current density change with the Hartmann number which is the key governing parameter. We also wish to assess changes in these physical variables with the parameter

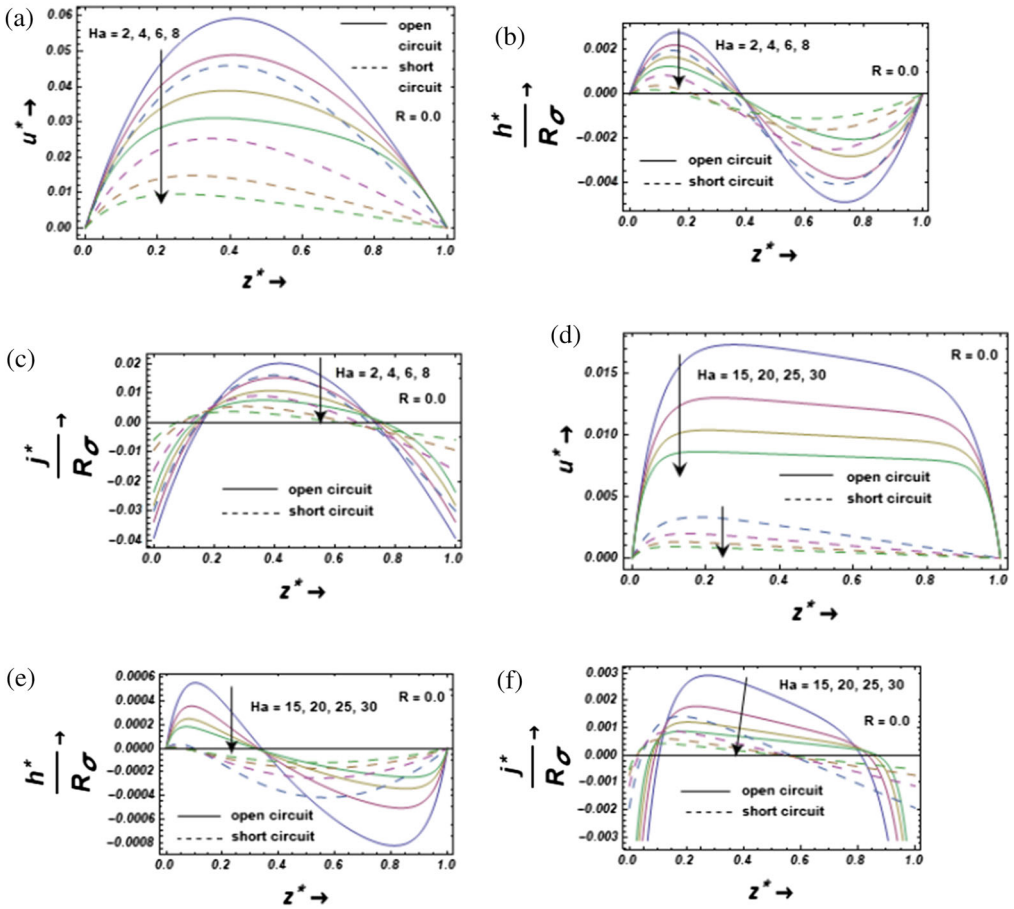

Figure 2. **(a)** Velocity profiles for various Hartmann numbers at $R = 0$, **(b)** induced magnetic field profiles for various Hartmann numbers at $R = 0$, **(c)** induced current density profiles for various Hartmann numbers at $R = 0$, **(d)** velocity profiles for various high Hartmann numbers at $R = 0$, **(e)** induced magnetic field profiles for various high Hartmann numbers at $R = 0$ and **(f)** induced current density profiles for various high Hartmann numbers at $R = 0$.

R by considering either asymmetrical heating ($R \neq 1$) or symmetrical heating ($R = 1$) of both walls.

Figure 2 shows the relative effects of magnetic field strength on the variables. In figures 2a–2c, the variations of fluid velocity, induced magnetic field and induced current density for small Hartmann number ($2 \leq Ha \leq 8$) are shown while figures 2d–2f show their counterparts for relatively large Hartmann number ($15 \leq Ha \leq 30$). All graphs in figure 2 correspond to the case $R = 0$ (asymmetrical heating). Also, to compare the results for the open- and short-circuit arrangements, in each plot, we have included dotted curves representing the short-circuit arrangement, and continuous curves representing the open-circuit case.

To assess the variation of the physical variables for the case of symmetric heating ($R = 1$), we have shown in figures 3a–3f the counterparts of figures 2a–2f when the two bounding vertical plates are maintained at the same uniform temperature.

We shall now discuss the significance of various plots given in figures 2 and 3 to highlight some interesting observations relating to our field variables *vis-à-vis* the physical parameters governing the flow. Consider figures 2a–2f for $R = 0$, which correspond to the asymmetric heating of the two bounding vertical walls. From these figures, it is worth noting that the fluid velocity for both open- and short-circuit cases, across any transverse cross-section of the channel, decreases with an increase in the value of the Hartmann number Ha. This observation is in line with the physical fact that externally applied magnetic fields are known to check the fluid flow. Also, it is quite interesting to note that the values of velocity for the open-circuit case are higher than the corresponding values for the short-circuit case for both low and relatively higher values of Ha, although this distinction is more pronounced for higher values of Ha. Furthermore, it is quite striking to see that the effect of higher values of Ha ($15 \leq Ha \leq 30$) is to flatten the velocity profiles (see figure 2d) in

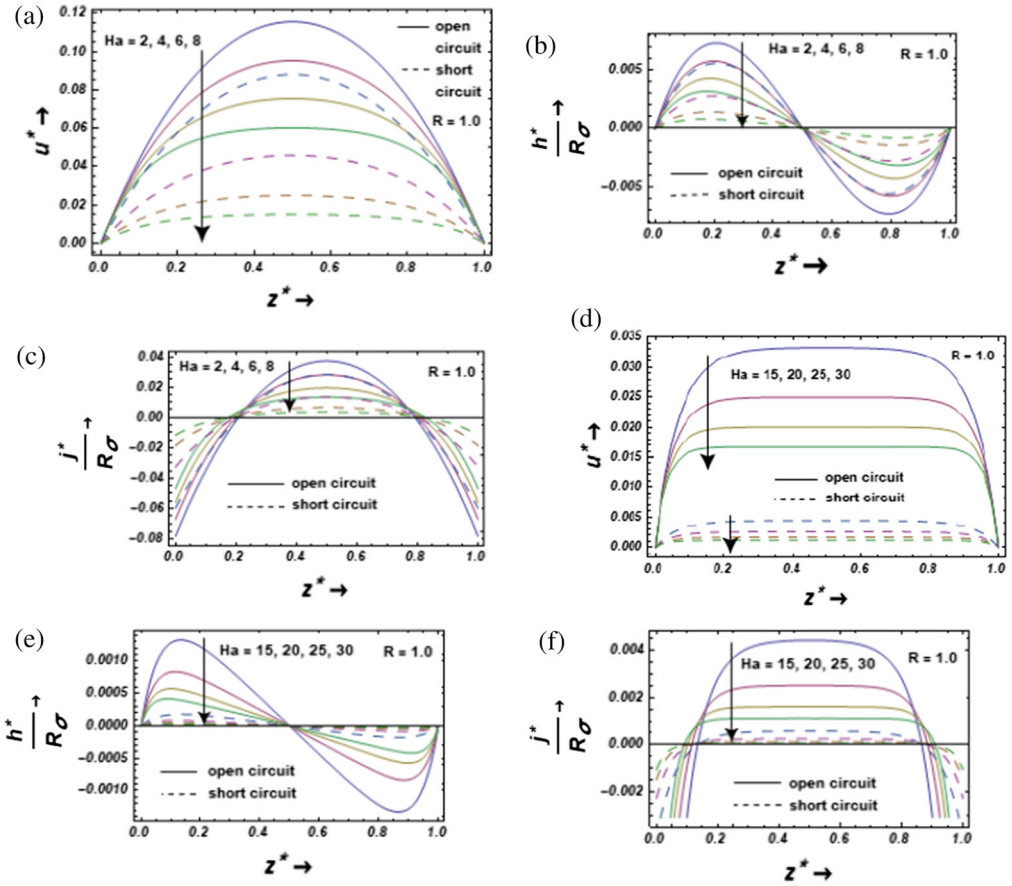

Figure 3. **(a)** Velocity profiles for various Hartmann numbers at $R = 1$, **(b)** induced magnetic field profiles for various Hartmann numbers at $R = 1$, **(c)** induced current density profiles for various Hartmann numbers at $R = 1$, **(d)** velocity profiles for various high Hartmann numbers at $R = 1$, **(e)** induced magnetic field profiles for various high Hartmann numbers at $R = 1$ and **(f)** induced current density profiles for various high Hartmann numbers at $R = 1$.

the central region of any transverse cross-section; this flattening phenomenon is more conspicuous for open-circuit velocity profiles.

As regards the induced magnetic field profiles shown in figures 2b and 2e, we can easily note different patterns compared to the ones for velocity profiles. For smaller values of Ha $(2 \leq Ha \leq 8)$, the magnetic profiles for both open and short circuits show a broadly similar pattern: the induced magnetic field first increases from its zero value to its maximum value and then falls back to its zero value in a region close to the left boundary ($z \approx 0.4$) before reversing its course to pass through a minimum (i.e., a negative value of the induced magnetic field) in the other part of the cross-section ($0.4 \approx z \leq 1$). During this cycle of fluctuation – i.e., passage through a maximum (positive value) and a minimum (negative value) – it is noticed that the absolute value of the induced magnetic field for the open-circuit case is higher than the corresponding value for the short circuit case at any point of a cross-section. For higher values of the Hartmann number $(15 \leq Ha \leq 30)$, we notice that the pattern for induced magnetic field profiles for the open-circuit case (continuous curves in figure 2e) is quite similar to the one reported above when Ha is relatively smaller. However, the corresponding relatively flattened profiles for the short-circuit case are in the negative domain of the induced magnetic field, thus showing attainment of minimum value. In other words, similar to our observations for the velocity plots, short-circuit case profiles of the induced magnetic field are relatively more sensitive to changes in the values of the applied magnetic field.

We now turn our attention to assess how induced current density profiles, shown in figures 2c and 2f, behave with Hartmann number Ha at any cross-section of the channel. It is quite interesting to note that induced current density values near either bounding wall, are negative for both open- and short-circuit cases.

Other than this, these profiles are broadly similar to the velocity profiles for both small and relatively larger values of the applied magnetic field. Moreover, similar to our earlier observations on the induced

Table 1. Skin friction and volumetric flow rate: Effect of Ha for asymmetric and symmetric heating of walls.

		Open circuit		Short circuit			
R	Ha	$(\tau)_{z=0}$	$(\tau)_{z=1}$	$(\tau)_{z=0}$	$(\tau)_{z=1}$	Open circuit Q	Short circuit Q
0.0	2.0	0.3283	−0.1717	0.2687	−0.1121	0.0391	0.0298
	4.0	0.3172	−0.1828	0.1877	−0.0533	0.0336	0.0162
	6.0	0.3060	−0.1940	0.1389	−0.0270	0.0280	0.0093
	8.0	0.2969	−0.2031	0.1094	−0.0155	0.0235	0.0059
1.0	2.0	0.5000	−0.5000	0.3808	−0.3808	0.0783	0.0596
	4.0	0.5000	−0.5000	0.2410	−0.2410	0.0672	0.0324
	6.0	0.5000	−0.5000	0.1658	−0.1658	0.0560	0.0186
	8.0	0.5000	−0.5000	0.1249	−0.1249	0.0469	0.0117

magnetic profiles, the absolute values of the induced current density for the open-circuit cases are larger than their short-circuit counterparts at any point of a transverse cross-section of the vertical channel.

Finally, to determine the differences in the profiles of our field variables when R changes from 0 (asymmetric heating case) to 1 (symmetric heating case), we have included counterparts of all plots in figure 2 for the case of symmetric heating. These profiles are given in figure 3. On close glance at the plots given in figures 2 and 3, one finds that for the typical values of the parameter R ($R = 0$ and 1) used in this analysis, velocity, induced magnetic field and induced current density profiles for both asymmetric and symmetric heating are strikingly similar save for magnitudes of these variables. However, some subtle differences can be noticed in deeper analysis. For instance, one may note that the symmetric current density profiles shown in figure 3f correspond to symmetric heating and how they are changed due to asymmetric heating; the symmetric and largely flat-in-the-middle current density profiles are easily displaced and become quite non-symmetric by asymmetric heating of the plate as can be seen in figure 2f.

As mentioned in the previous section, some of the engineering quantities of interest, namely, the wall shear stress at the bounding surfaces and the flow rates through a cross-section of the vertical channel, play important roles in practical applications in a wide range of industries. Thus, in table 1 we have included computed values of these two quantities for both open-circuit and short-circuit arrangements showing their variations with governing parameters R and Ha. It is quite interesting to note that for symmetric heating configuration, the skin friction values at either wall for the open-circuit arrangement are insensitive to changes in the Hartmann number Ha while their absolute values show a marked reduction with increasing Ha for short-circuit case. For the asymmetric heating ($R = 0$), one may note the decrease in the absolute values of skin friction at either plate with an increase in Ha for the short-circuit case. However, for the open-circuit arrangement, absolute values of the skin friction on the left wall decrease with increasing Ha while the opposite happens on the right wall. As regards volume flow rate, it is quite apparent that the flow rate values for the open-circuit case are fairly larger than their counterparts for the short-circuit case for both symmetric and asymmetric heating. However, concerning changes in Ha, from 2 to 8, the volume flow rate is larger for symmetric heating than their counterparts for the asymmetric heating case.

5. Conclusions

We have obtained exact solution of the model equations, to see the effect of induced magnetic field on the hydromagnetic free convective flow of an electrically conducting liquid between the vertical channels. The effect of Hartmann number for both open and short circuits has been examined on the velocity, induced magnetic field, induced current density, skin friction and mass flow rate. The following conclusions are drawn from the present study:

- The velocity, induced current density and induced magnetic field have decreasing tendency with increasing values of Hartmann number for both open- and short-circuit cases.
- For the open-circuit case, velocity, induced magnetic field and induced current density are higher than that for the short-circuit component.
- The values of velocity, induced magnetic field and induced current density for the symmetric case are higher than that for the asymmetric case in both cases of circuit arrangements.
- The influence of Ha is to decrease the mass flow rate for both open and short circuits.
- It is worth mentioning that since our flow is laminar with a moderate Ha, it is seemingly stable for both circuits.

Acknowledgements

One of the authors (Naveen Dwivedi) acknowledges the financial support in the form of a Senior Research Fellowship (UGC Ref. No. 1274/PWD) from the University Grants Commission, New Delhi, India.

References

[1] E M Sparrow and R D Cess, *Int. J. Heat Mass Transf.* **1**, 267 (1961)
[2] N C Sacheti, P Chandran and A K Singh, *Int. Commun. Heat Mass Transf.* **21**, 131 (1994)
[3] P Chandran, N C Sacheti and A K Singh, *J. Phys. Soc. Jpn* **67**, 124 (1998)
[4] R M Singer, *J. Appl. Math. Phys*. **16**, 483 (1995)
[5] A J Chamkha, *Int. J. Eng. Sci.* **35**, 975 (1997)
[6] C Y Han, *Int. J. Heat Mass Transf.* **52**, 5895 (2009)
[7] J C Umavathi and I C Liu, *Meccanica* **48**, 2221 (2013)
[8] B K Jha and C A Apere, *J. Heat Transfer* **133**, 12 (2011)
[9] B K Jha, B Aina and A T Ajiya, *Ain Shams Eng. J.* **6**, 289 (2015)
[10] M Sheikholeslami, T Hayat and A. Alsaedi, *Int. J. Heat Mass Transf.* **96**, 513 (2016)
[11] N Dwivedi, A K Singh and A Kumar, *Int. J. Appl. Comput. Math.* **5**, 75 (2019)
[12] N Dwivedi and A K Singh, *Heat Transf.-Asian Res.* **49**, 1402 (2020)
[13] N Dwivedi and A K Singh, *Pramana – J. Phys.* **94**, 142 (2020)
[14] P Mathur and S R Mishra, *Pramana – J. Phys.* **94**, 69 (2020)
[15] S Ghosh and S Mukhopadhyay, *Pramana – J. Phys.* **94**, 61 (2020)
[16] S Globe, *Phys. Fluids* **2**, 404 (1959)
[17] J T Yen, *J. Heat Transfer* **85**, 371 (1963)
[18] K L Arora and P R Gupta, *Phys. Fluids* **15**, 1146 (1971)
[19] M Guria, B K Das, R N Jana and S K Ghosh, *Int. J. Fluid Mech. Res.* **34**, 521 (2007)
[20] R K Singh, A K Singh, N C Sacheti and P Chandran, *Heat Mass Transfer* **46**, 523 (2010)
[21] S K Ghosh, O A Beg and J Zueco, *Meccanica* **14**, 175 (2010)
[22] R K Singh and A K Singh, *Acta Mech. Sin.* **28**, 315 (2012)
[23] N S Akbar, M Raza and R Ellahi, *Eur. Phys. J. Plus* **129**, 155 (2014)
[24] B K Jha and B Aina, *Alex. Eng. J.* **55**, 2087 (2016)
[25] B K Jha and B Aina, *J. Nanofluids* **6**, 1 (2017)
[26] B K Jha and B Aina, *Commun. Nonlinear Sci. Numer. Simulat.* **64**, 14 (2018)
[27] Z Iqbal and Z. Mahmood, *Arab. J. Sci. Eng.* **44**, 873 (2019)
[28] S Shaiq and E N Maraj, *Arab. J. Sci. Eng.* **44**, 7515 (2019)
[29] N Dwivedi and A K Singh, *Proc. Natl. Acad. of Sci., India Sect. A: Phys. Sci.,* https://doi.org/10.1007/s40010-020-00720-x (2020)
[30] N Dwivedi and A K Singh, *Indian J. Phys.,* https://doi.org/10.1007/s12648-020-01953-7 (2021)
[31] J F Osterle and F J Young, *J. Fluid Mech.* **1**, 512 (1961)
[32] G Poots, *Int. J. Heat Mass Transf.* **3**, 1 (1961)
[33] J C Umavathi, *Int. J. Non-Linear Mech.* **31**, 371 (1996)
[34] J C Umavathi, J P Kumar, R R Gorla and B J Gireesha, *Int. J. Appl. Mech. Eng.* **21**, 683 (2016)
[35] J H He, T S Amer, S Elnaggar and A A Galal, *Axioms* **10(3)**, 191 (2021)
[36] C H He, D Tian, G M Moatimid, H F Salman and M H Zekry, *J. Low Frequency Noise, Vibration and Active Control*, https://doi.org/10.1177/14613484211026407 (2021)
[37] J H He, G M Moatimid and D R Mostapha, *J. Electroanal. Chem.* **895**, 115388 (2021)
[38] Y Tian and J Liu, *Therm. Sci.* **25**, 2235 (2021)